

ROBUST BDDC PRECONDITIONERS FOR REISSNER-MINDLIN PLATE BENDING PROBLEMS AND MITC ELEMENTS

L. BEIRÃO DA VEIGA*, C. CHINOSI†, C. LOVADINA‡, AND L. F. PAVARINO§

Abstract. A Balancing Domain Decomposition Method by Constraints (BDDC) is constructed and analyzed for the Reissner-Mindlin plate bending problem discretized with MITC finite elements. This BDDC algorithm is based on selecting the plate rotations and deflection degrees of freedom at the subdomain vertices as primal continuity constraints. After the implicit elimination of the interior degrees of freedom in each subdomain, the resulting plate Schur complement is solved by the preconditioned conjugate gradient method. The preconditioner is based on the solution of local Reissner-Mindlin plate problems on each subdomain with clamping conditions at the primal degrees of freedom and on the solution of a coarse Reissner-Mindlin plate problem for the primal degrees of freedom. The main results of the paper are the proof and numerical verification that the proposed BDDC plate algorithm is scalable, quasi-optimal, and, most important, robust with respect to the plate thickness. While this result is due to an underlying mixed formulation of the problem, both the interface plate problem and the preconditioner are positive definite. The numerical results also show that the proposed algorithm is robust with respect to discontinuities of the material properties.

Key words. Domain Decomposition methods, BDDC, scalable preconditioners, Reissner-Mindlin model, plate bending problem, MITC finite elements

AMS subject classifications. 65N55

1. Introduction. The Reissner-Mindlin theory is widely used to describe the bending behavior of an elastic plate loaded by a transverse force. Despite its simple formulation, the discretization by means of finite elements is not straightforward, since standard low-order schemes exhibit a severe lack of convergence whenever the thickness is too small with respect to the other characteristic dimensions of the plate. This undesirable phenomenon, known as *shear locking*, is nowadays well understood: as the plate thickness tends to zero, the Reissner-Mindlin model enforces the Kirchhoff constraint, which is usually too severe at the discrete level (see, for instance, the monograph by Brezzi and Fortin [18]). The most popular way to overcome the shear locking phenomenon is to reduce the influence of the shear energy by considering a mixed formulation. As a consequence, the choice of the discrete spaces requires particular care, also because of the possible occurrence of *spurious modes*. In addition, *boundary layer effects* (see [3, 4]) may spoil the convergence rate of the method at hand. A vast engineering and mathematical literature is devoted to the design and the analysis of plate elements, see e.g. the works [2, 6, 7, 10, 19, 21, 22, 26, 29, 36, 37, 38, 39, 46, 47]. However, a limited number of domain decomposition works are available for the efficient iterative solution of plate problems.

The goal of this paper is to construct and analyze a Balancing Domain Decomposition Method by Constraints (BDDC) for the Reissner-Mindlin plate bending problem discretized with one of the most popular and efficient approach: the MITC finite

*Corresponding author. Dipartimento di Matematica, Università di Milano, Via Saldini 50, 20133 Milano, Italy. Email: beirao@mat.unimi.it, URL: <http://mat.unimi.it/~beirao/>

†Dipartimento di Scienze e Tecnologie Avanzate, Università del Piemonte Orientale, Via Bellini 25/G, I-15100 Alessandria, ITALY. Email: chinosi@mfn.unipmn.it, URL: <http://www.mfn.unipmn.it/~chinosi/>

‡Dipartimento di Matematica, Università di Pavia, Via Ferrata 1, 27100 Pavia, ITALY. Email: carlo.lovadina@unipv.it, URL: <http://www-dimat.unipv.it/lovadina/>

§Dipartimento di Matematica, Università di Milano, Via Saldini 50, 20133 Milano, ITALY. Email: pavarino@mat.unimi.it, URL: <http://mat.unimi.it/~pavarino/>

elements (see [8, 9, 17, 19]). Our BDDC algorithm is based on selecting the plate rotations and deflection degrees of freedom at the subdomain vertices as primal continuity constraints. The resulting BDDC preconditioner is built from the solutions of local Reissner-Mindlin plate problems on each subdomain with clamping conditions at the primal degrees of freedom and on the solution of a coarse Reissner-Mindlin plate problem for the primal degrees of freedom. The main results of the paper are the proof and numerical verification that our BDDC algorithm is scalable, quasi-optimal and, most important, robust with respect to the plate thickness. While this uniformity in the plate thickness is due to an underlying mixed formulation of the problem, both the interface plate problem and the BDDC preconditioner are positive definite. The numerical results also show that our algorithm is robust with respect to discontinuities of the material properties.

Introduced by Dohrmann [23] and analyzed by Mandel, Dohrmann and Tezaur [40, 41], BDDC methods have evolved from previous domain decomposition work on Balancing Neumann-Neumann methods. They are closely related to FETI-DP methods, see e.g. Farhat et al. [28], exhibiting essentially the same spectrum of the latter when the primal constraints are the same; see e.g. [34, 16]. We refer to the monograph by Toselli and Widlund [49, Ch. 6] for a detailed treatment of the relationships between Neumann-Neumann, FETI and FETI-DP algorithms. BDDC algorithm have been extended in recent years from scalar elliptic problems to almost incompressible elasticity (Dohrmann [24, 25]), the Stokes system (Li and Widlund [35]), flow in porous media (Tu [51]), spectral element discretizations (Pavarino [43]).

Previous domain decomposition work for plates focused on the Kirchhoff (biharmonic) plate problem (Le Tallec et al. [33], Brenner and Sung [13, 14, 15], Marcinkowski [42]), where C^1 or nonconforming finite elements are required and the plate thickness is not an issue. The Neumann-Neumann method proposed in [33] can be extended to thin plate and shell models, but the resulting convergence rate depends on the thickness parameter. Arnold et al. [5] considered the Reissner-Mindlin plate model, but a mixed formulation was used in order to avoid locking when the plate thickness approaches zero and block preconditioners were used for the resulting saddle point discrete problem, with blocks derived from preconditioners for simpler subproblems. In our approach instead, we attack directly the symmetric positive definite Reissner-Mindlin plate model, in the spirit of our previous work [12] for almost incompressible elasticity, and solve iteratively the resulting Schur complement problem by a conjugate gradient method with our scalable BDDC plate preconditioner.

The rest of the paper is organized as follows. In Section 2, we present the Reissner-Mindlin plate bending problem and its discretization with MITC finite elements. The basic substructuring procedure is introduced in Section 3, while the BDDC algorithm is introduced in Section 4. The theoretical analysis of the BDDC uniform scalability is developed in Section 5, while the results of several numerical experiments are presented in Section 6. The Appendix in Section 7 contains two technical Lemmata needed in the analysis of Section 5.

2. The MITC Reissner-Mindlin plate bending problem. Let Ω be a polygonal domain in \mathbb{R}^2 representing the midsurface of the plate. For simplicity of exposition, we assume that the plate is clamped on the whole boundary $\partial\Omega$, although what follows extends identically to more general cases. Following the Reissner-Mindlin

model, see for instance [8], the plate bending problem requires to solve

$$\begin{cases} \text{Find } \boldsymbol{\theta}^{ex} \in [H_0^1(\Omega)]^2, u^{ex} \in H_0^1(\Omega) \text{ such that} \\ a(\boldsymbol{\theta}^{ex}, \boldsymbol{\eta}) + \mu k t^{-2} (\boldsymbol{\theta}^{ex} - \nabla u^{ex}, \boldsymbol{\eta} - \nabla v) = (f, v) \quad \forall \boldsymbol{\eta} \in [H_0^1(\Omega)]^2, v \in H_0^1(\Omega), \end{cases} \quad (2.1)$$

where μ is the shear modulus and k is the so-called shear correction factor. Above, t represents the plate thickness, u^{ex} the deflection, $\boldsymbol{\theta}^{ex}$ the rotation of the normal fibers and f the applied scaled normal load. Moreover, (\cdot, \cdot) stands for the standard scalar product in $L^2(\Omega)$ and the bilinear form $a(\cdot, \cdot)$ is defined by

$$a(\boldsymbol{\theta}^{ex}, \boldsymbol{\eta}) = (\mathbb{C}\boldsymbol{\varepsilon}(\boldsymbol{\theta}^{ex}), \boldsymbol{\varepsilon}(\boldsymbol{\eta})),$$

with \mathbb{C} the positive definite tensor of bending moduli. Introducing the scaled shear stresses $\boldsymbol{\gamma}^{ex} = \mu k t^{-2} (\boldsymbol{\theta}^{ex} - \nabla u^{ex})$, Problem (2.1) can be written in terms of the following mixed variational formulation:

$$\begin{cases} \text{Find } \boldsymbol{\theta}^{ex} \in [H_0^1(\Omega)]^2, u^{ex} \in H_0^1(\Omega), \boldsymbol{\gamma}^{ex} \in [L^2(\Omega)]^2 \text{ such that} \\ a(\boldsymbol{\theta}^{ex}, \boldsymbol{\eta}) + (\boldsymbol{\gamma}^{ex}, \boldsymbol{\eta} - \nabla v) = (f, v) \quad \forall \boldsymbol{\eta} \in [H_0^1(\Omega)]^2, v \in H_0^1(\Omega) \\ (\boldsymbol{\theta}^{ex} - \nabla u^{ex}, \boldsymbol{s}) - \frac{t^2}{\mu k} (\boldsymbol{\gamma}^{ex}, \boldsymbol{s}) = 0 \quad \forall \boldsymbol{s} \in [L^2(\Omega)]^2. \end{cases} \quad (2.2)$$

To simplify notation, and without any loss of generality, we will assume $\mu k = 1$ in the analysis that follows.

2.1. Discretization of the problem with the MITC elements. We will now present the discretization of the problem following the MITC (Mixed Interpolation of Tensorial Components) elements. Since the MITC is a large family of elements, we will keep a general standpoint without detailing the particular description of the discrete spaces and operators, which depend on the particular MITC element chosen; a list of elements can be found for instance in [8, 9, 19]. In Section 6, we will detail the MITC 9 element, which is the one used in our numerical tests.

Let τ_h denote a triangular or quadrilateral conforming finite element mesh on Ω , of characteristic mesh size h . Let $\boldsymbol{\Theta}$, U and $\boldsymbol{\Gamma}$ represent the discrete spaces for rotations, deflections and shear stresses, respectively. In the sequel, we will set the compact notation $\mathbf{X} = \boldsymbol{\Theta} \times U$. Then the Reissner-Mindlin plate bending problem (2.2) discretized with MITC elements reads

$$\begin{cases} \text{Find } (\boldsymbol{\theta}, u) \in \mathbf{X}, \boldsymbol{\gamma} \in \boldsymbol{\Gamma} \text{ such that} \\ a(\boldsymbol{\theta}, \boldsymbol{\eta}) + (\boldsymbol{\gamma}, \Pi \boldsymbol{\eta} - \nabla v) = (f, v) \quad \forall (\boldsymbol{\eta}, v) \in \mathbf{X} \\ (\Pi \boldsymbol{\theta} - \nabla u, \boldsymbol{s}) - t^2 (\boldsymbol{\gamma}, \boldsymbol{s}) = 0 \quad \forall \boldsymbol{s} \in \boldsymbol{\Gamma}, \end{cases} \quad (2.3)$$

where $\Pi : ([H^1(\Omega)]^2 + \boldsymbol{\Gamma}) \longrightarrow \boldsymbol{\Gamma}$ is the MITC reduction operator. Using the second equation of (2.3), shear stresses can be eliminated to obtain the following positive definite discrete formulation:

$$\begin{cases} \text{Find } (\boldsymbol{\theta}, u) \in \mathbf{X} \text{ such that} \\ b((\boldsymbol{\theta}, u), (\boldsymbol{\eta}, v)) = (f, v) \quad \forall (\boldsymbol{\eta}, v) \in \mathbf{X}, \end{cases} \quad (2.4)$$

where we have introduced the compact notation

$$b((\boldsymbol{\theta}, u), (\boldsymbol{\eta}, v)) := a(\boldsymbol{\theta}, \boldsymbol{\eta}) + t^{-2} (\Pi \boldsymbol{\theta} - \nabla u, \Pi \boldsymbol{\eta} - \nabla v). \quad (2.5)$$

The MITC spaces and the associated operator Π are well known to satisfy the following five properties, which will play a key role in the sequel. In what follows, $Q \subset L^2(\Omega)$ represents an ad hoc discrete auxiliary space. For the proofs of these properties, see [9, 19].

P1. $\nabla W \subset \mathbf{\Gamma}$.

P2. $\text{curl } \mathbf{\Gamma} \subset Q$.

P3. $\text{curl } \Pi \boldsymbol{\eta} = P \text{curl } \boldsymbol{\eta}$, $\boldsymbol{\eta} \in [H_0^1]^2$, where $P : L^2 \rightarrow Q$ denotes the L^2 projection.

P4. $\{\boldsymbol{\gamma} \in \mathbf{\Gamma} : \text{curl } \boldsymbol{\gamma} = 0\} = \nabla W_h$.

P5. $(\boldsymbol{\Theta}, Q)$ is a stable pair of spaces for the Stokes problem.

We will also require the following additional property to hold, see [10].

P6. For every edge l of the mesh, denote with $\boldsymbol{\tau}$ its tangent vector. We assume that the combined operator $(\Pi \boldsymbol{\theta}|_l) \cdot \boldsymbol{\tau}$ depends only on $\boldsymbol{\theta}|_l \cdot \boldsymbol{\tau}$ for all $\boldsymbol{\theta} \in \boldsymbol{\Theta}$. Therefore the above combined operator is well defined also when applied to functions living only on edges.

Note that in this paper we address directly the positive definite Problem (2.4), in the spirit of [12], instead of the mixed formulation. A vast literature exists on the convergence analysis of the MITC elements, see for instance [9, 19, 26, 45] and also [11, 27]. The MITC elements perform optimally with respect to the polynomial degree and regularity of the solution, and their rate of convergence is independent of the thickness parameter t .

3. Iterative substructuring. We decompose the domain Ω into N open, non-overlapping subdomains Ω_i of characteristic size H forming a shape-regular finite element mesh τ_H . This coarse triangulation τ_H is further refined into a finer triangulation τ_h of characteristic size h ; both meshes will typically be composed of triangles or quadrilaterals. In the sequel, we assume that the material tensor \mathbb{C} is constant constant through the whole domain; see Remark 5.2.

As it is standard in iterative substructuring methods, we first reduce the problem to the interface

$$\Gamma = \left(\bigcup_{i=1}^N \partial\Omega_i \right) \setminus \partial\Omega,$$

by implicitly eliminating the interior degrees of freedom, a process also known as static condensation. In variational form, this process consists in a suitable decomposition of the discrete space $\mathbf{X} = \boldsymbol{\Theta} \times U$. More precisely, let us define $\mathbf{W} = \mathbf{X}|_\Gamma$, i.e. the space of the traces of functions in \mathbf{X} , as well as the local spaces

$$\mathbf{X}_i = \mathbf{X} \cap [H_0^1(\Omega_i)]^3. \quad (3.1)$$

The space \mathbf{X} can be decomposed as

$$\mathbf{X} = \oplus_{i=1}^N \mathbf{X}_i \oplus \overline{\mathcal{H}}(\mathbf{W}).$$

Here $\overline{\mathcal{H}} : \mathbf{W} \rightarrow \mathbf{X}$ is the discrete "plate-harmonic" extension operator defined by solving the problem

$$\begin{cases} \text{Find } \overline{\mathcal{H}}(\mathbf{w}_\Gamma) \in \mathbf{X} \text{ such that:} \\ b(\overline{\mathcal{H}}(\mathbf{w}_\Gamma), \mathbf{v}_I) = 0 \quad \forall \mathbf{v}_I \in \mathbf{X}_i \quad i = 1, 2, \dots, N \\ \overline{\mathcal{H}}(\mathbf{w}_\Gamma)|_\Gamma = \mathbf{w}_\Gamma. \end{cases} \quad (3.2)$$

Defining the Schur complement bilinear form

$$s(\mathbf{w}_\Gamma, \mathbf{v}_\Gamma) = b(\overline{\mathcal{H}}(\mathbf{w}_\Gamma), \overline{\mathcal{H}}(\mathbf{v}_\Gamma)), \quad (3.3)$$

it follows that the interface component of the discrete solution satisfies the reduced system

$$s(\mathbf{u}_\Gamma, \mathbf{v}_\Gamma) = \langle \tilde{\mathbf{f}}, \mathbf{v}_\Gamma \rangle \quad \forall \mathbf{v}_\Gamma \in \mathbf{W}, \quad (3.4)$$

for a suitable right-hand side $\tilde{\mathbf{f}}$. In order to simplify the notation, in the sequel we will drop the index Γ for functions in \mathbf{W} if there is no risk of confusion. Moreover, in the rest of the contribution C will indicate a general scalar constant, independent of H and h , which may change on different occurrences.

4. A Balancing Domain Decomposition method by Constraints. The BBDC preconditioner, introduced by Dohrmann [23] and analyzed by Mandel and Dohrmann [40], applies to the classical Schur complement system and can be regarded as an evolution of the Balancing Neumann-Neumann preconditioner. In this section we introduce the BBDC preconditioner of Ref. [23, 40], formulated with the notation of Ref. [49]. We need a set of preliminary definitions.

In the sequel we indicate with

$$\Gamma_i := \partial\Omega_i \cap \Gamma,$$

while Γ_{ij} , $i, j \in \{1, 2, \dots, N\}$, will represent the common edge between two adjacent domains Ω_i and Ω_j .

We introduce the local spaces $\overline{\mathbf{W}}_i$ as the spaces of discrete functions defined on $\overline{\mathbf{W}}_i = \mathbf{W}|_{\partial\Omega_i}$, $i = 1, 2, \dots, N$. Let $\overline{\mathcal{H}}_i : \overline{\mathbf{W}}_i \rightarrow \mathbf{X}|_{\Omega_i}$, $i = 1, 2, \dots, N$, represent the restriction of the operator $\overline{\mathcal{H}}$ to the domain Ω_i

$$\begin{cases} \text{Find } \overline{\mathcal{H}}_i(\mathbf{w}_i) \in \mathbf{X}|_{\Omega_i} \text{ such that:} \\ b_i(\overline{\mathcal{H}}_i(\mathbf{w}_i), \mathbf{v}_i) = 0 \quad \forall \mathbf{v}_i \in \mathbf{X}_i \\ \overline{\mathcal{H}}_i(\mathbf{w}_i)|_{\Gamma_i} = \mathbf{w}_i. \end{cases} \quad (4.1)$$

where the $b_i(\cdot, \cdot)$ are given by restricting the integrals in $b(\cdot, \cdot)$ to the domain Ω_i , $i = 1, 2, \dots, N$.

We then define the local bilinear forms on the space $\overline{\mathbf{W}}_i$

$$s_i(\mathbf{w}_i, \mathbf{v}_i) = b_i(\overline{\mathcal{H}}_i \mathbf{w}_i, \overline{\mathcal{H}}_i \mathbf{v}_i), \quad \forall \mathbf{w}_i, \mathbf{v}_i \in \overline{\mathbf{W}}_i, \quad (4.2)$$

For simplicity, we adopt the shortened notation

$$s_i(\mathbf{w}_i) := s_i(\mathbf{w}_i, \mathbf{w}_i) \quad \forall \mathbf{w}_i \in \overline{\mathbf{W}}_i,$$

and the same for all the other bilinear forms appearing in the paper.

Furthermore, let the prolongation operators R_i^T , $i = 1, 2, \dots, N$ be maps which extend any function of $\overline{\mathbf{W}}_i$ to the function of \mathbf{W} which is zero at all the nodes not in $\partial\Omega_i \cap \Gamma$. Conversely, we call R_i , $i = 1, 2, \dots, N$, the restriction operators $\mathbf{W} \rightarrow \overline{\mathbf{W}}_i$ that leave the function unchanged on Γ_i . Note that, by definition of the s_i , it holds

$$\sum_{i=1}^N s_i(R_i \mathbf{w}, R_i \mathbf{v}) = s(\mathbf{w}, \mathbf{v}) \quad \forall \mathbf{w}, \mathbf{v} \in \mathbf{W}. \quad (4.3)$$

We also need the following definition (see for example Section 6.2.1 of Ref. [49]). Given any node $x \in \Gamma$, define $N_x = \#\{j \in \mathbb{N} \mid x \in \partial\Omega_j\}$. Then, the weighted counting operators $\delta_i : \overline{\mathbf{W}}_i \rightarrow \overline{\mathbf{W}}_i$ (and their inverse operators δ_i^\dagger) are defined by

$$\begin{aligned} \delta_i \mathbf{v}_i(x) &= N_x \mathbf{v}_i(x) \quad \forall x \text{ node of } \partial\Omega_i \cap \Gamma \\ \delta_i^\dagger \mathbf{v}_i(x) &= N_x^{-1} \mathbf{v}_i(x) \quad \forall x \text{ node of } \partial\Omega_i \cap \Gamma . \end{aligned} \quad (4.4)$$

Let the local constraint operators $C_i : \overline{\mathbf{W}}_i \rightarrow \mathbb{R}^{3cc_i}$ be the operators that read the function values at the corners of the subdomain Ω_i , with cc_i the number of corners of the subdomain. Then the local constrained spaces are

$$\mathbf{W}_i = \{\mathbf{w}_i \in \overline{\mathbf{W}}_i \mid C_i \mathbf{w}_i = \mathbf{0}\} . \quad (4.5)$$

We will moreover introduce a global coarse space $\mathbf{W}_0 \subset \mathbf{W}$, whose degrees of freedom are the function values at the subdomain corner nodes. Given the number m of such subdomain corners, let $w_c \in \mathbb{R}^{3m}$ be a vector representing the respective nodal values. Then the space \mathbf{W}_0 is defined by

$$\mathbf{W}_0 = \left\{ \sum_{i=1}^N R_i^T \delta_i^\dagger \mathbf{w}_{0,i} \mid C_i \mathbf{w}_{0,i} = R_i^C w_c, w_c \in \mathbb{R}^{3m}, s_i(\mathbf{w}_{0,i}, \mathbf{w}_{0,i}) \rightarrow \min \right\}, \quad (4.6)$$

where R_i^C is the operator that extracts the corner node values for the subdomain Ω_i from the global vector w_c of all the subdomain corner node values.

Any element $\mathbf{w} \in \mathbf{W}$ can be uniquely decomposed as

$$\mathbf{w} = \mathbf{w}_0 + \sum_{i=1}^N \mathbf{w}_i, \quad \mathbf{w}_0 \in \mathbf{W}_0, \quad \mathbf{w}_i \in \mathbf{W}_i \text{ for } i = 1, \dots, N . \quad (4.7)$$

Let the inexact bilinear forms, see (4.6), be defined by

$$\begin{aligned} \tilde{s}_0(\mathbf{w}_0, \mathbf{v}_0) &= \sum_{i=1}^N s_i(\mathbf{w}_{i,0}, \mathbf{v}_{i,0}) \quad \forall \mathbf{w}_0, \mathbf{v}_0 \in \mathbf{W}_0, \\ \tilde{s}_i(\mathbf{w}_i, \mathbf{v}_i) &= s_i(\delta_i \mathbf{w}_i, \delta_i \mathbf{v}_i) \quad \forall \mathbf{w}_i, \mathbf{v}_i \in \mathbf{W}_i, \quad i = 1, 2, \dots, N . \end{aligned} \quad (4.8)$$

Finally, we define the coarse operator $P_0 : \mathbf{W} \rightarrow \mathbf{W}_0$ by

$$\tilde{s}_0(P_0 \mathbf{u}, \mathbf{v}_0) = s(\mathbf{u}, \mathbf{v}_0) \quad \forall \mathbf{v}_0 \in \mathbf{W}_0, \quad (4.9)$$

and the local operators $P_i = R_i^T \tilde{P}_i : \mathbf{W} \rightarrow R_i^T \mathbf{W}_i$ by

$$\tilde{s}_i(\tilde{P}_i \mathbf{u}, \mathbf{v}_i) = s(\mathbf{u}, R_i^T \mathbf{v}_i) \quad \forall \mathbf{v}_i \in \mathbf{W}_i. \quad (4.10)$$

Then, our BDDC method is defined by the preconditioned operator

$$P = \sum_{i=0}^N P_i . \quad (4.11)$$

5. Uniform scalability of the BBDC preconditioned operator. In this section, we bound the condition number of the preconditioned BBDC operator P introduced in (4.11). We start by briefly re-stating the general results for BBDC preconditioners of Ref. [40] and presenting our condition number bound for P . In the following Section 5.1, we will present a partially different proof for the general results of Ref. [40]. Our proof follows the setting and notations of Ref. [49], which better fit our purposes. The main novelty lays in Section 5.2, where we will address the following fundamental Assumption 5.1 for the MITC plate bending elements:

ASSUMPTION 5.1. *Given any Γ_i , $i = 1, 2, \dots, N$, let \mathcal{E}_i represent the set of the edges of Γ_i . Then, we assume that there exist two positive constants k_* , k^* and a boundary seminorm $|\cdot|_{\tau(\Gamma_i)}$ on $\overline{\mathbf{W}}_i$, $i = 1, 2, \dots, N$, such that*

$$|\mathbf{w}_i|_{\tau(\Gamma_i)}^2 \leq k^* s_i(\mathbf{w}_i) \quad \forall \mathbf{w}_i \in \overline{\mathbf{W}}_i ; \quad (5.1)$$

$$|\mathbf{w}_i|_{\tau(\Gamma_i)}^2 \geq k_* s_i(\mathbf{w}_i) \quad \forall \mathbf{w}_i \in \mathbf{W}_i ; \quad (5.2)$$

$$|\mathbf{w}_i|_{\tau(\Gamma_i)}^2 = \sum_{e \in \mathcal{E}_i} |\mathbf{w}_i|_{\tau(e)}^2 \quad \forall \mathbf{w}_i \in \overline{\mathbf{W}}_i , \quad (5.3)$$

where $|\cdot|_{\tau(e)}$ is a given seminorm on the edge e .

We notice that we cannot adopt the obvious choice $|\mathbf{w}_i|_{\tau(\Gamma_i)} = s_i(\mathbf{w}_i)$, since it can be shown that it does not satisfy (5.3), not even with a bound up to a uniform constant. The following theorems are the main theoretical results of the paper.

THEOREM 5.1. *If Assumption 5.1 holds, then the condition number of the preconditioned operator P in (4.11) satisfies the bound*

$$\text{Cond}(P) \leq C(1 + 5k_*^{-1}k^*).$$

The proof of this result is presented in the following Section 5.1.

THEOREM 5.2. *The constants k_* and k^* of Assumption 5.1 are bounded by*

$$k^* \leq C_1, \quad k_*^{-1} \leq C_2 \frac{H}{h},$$

with constants C_1, C_2 depending only on the material constants and mesh regularity. Therefore, we have the convergence rate bound

$$\text{Cond}(P) \leq C \left(1 + \frac{H}{h} \right),$$

with the constant C depending only on the material constants and mesh regularity.

The proof of this result is given in the following Section 5.2.

REMARK 5.1. *The numerical experiments presented in Sec. 6 seem to indicate that a sharper (poly)logarithmic bound might hold, at least for the simple geometry considered in the tests.*

REMARK 5.2. *Since the proofs presented in this paper are already quite technical, we refrain from a theoretical study of the condition number behavior in the presence of jumps for the material constants. The numerical tests presented in Section 6 show a very robust behavior also in this respect.*

5.1. Proof of Theorem 5.1. In this section we prove Theorem 5.1. We modify the proof shown in Ref. [40] following the theoretical setting of Ref. [49], Section 2.3, since we believe this may allow for a clearer understanding of the results. We start showing the following three lemmata.

LEMMA 5.3. *There exists a constant C_0 such that every $\mathbf{w} \in \mathbf{W}$ admits a decomposition*

$$\mathbf{w} = \mathbf{w}_0 + \sum_{i=1}^N R_i^T \mathbf{w}_i \quad \mathbf{w}_i \in \mathbf{W}_i, \quad i = 0, 1, \dots, N \quad (5.4)$$

that satisfies

$$\sum_{i=0}^N \tilde{s}_i(\mathbf{w}_i) \leq C_0^2 s(\mathbf{w}) . \quad (5.5)$$

It holds $C_0^2 = 5$.

Proof. Given $\mathbf{w} \in \mathbf{W}$, let $\mathbf{w}_0 = \sum_{i=1}^N R_i^T \delta_i^\dagger \mathbf{w}_{0,i}$ be the unique function in \mathbf{W}_0 such that $C_i \mathbf{w}_{0,i} = C_i R_i \mathbf{w}$. Then set

$$\mathbf{w}_i = \delta_i^\dagger (R_i \mathbf{w} - \mathbf{w}_{0,i}) . \quad (5.6)$$

From the definition of the operators δ_i^\dagger in (4.4) it easily follows

$$\sum_{i=1}^N R_i^T \delta_i^\dagger R_i \mathbf{v} = \mathbf{v} \quad \forall \mathbf{v} \in \mathbf{W} . \quad (5.7)$$

As a consequence of (5.7) and the above definitions we have

$$\mathbf{w}_0 + \sum_{i=1}^N R_i^T \mathbf{w}_i = \mathbf{w}_0 + \sum_{i=1}^N R_i^T \delta_i^\dagger (R_i \mathbf{w} - \mathbf{w}_{0,i}) = \mathbf{w} , \quad (5.8)$$

which is identity (5.4). From the definitions (5.6), (4.8), some basic algebra and identity (4.3) it follows

$$\begin{aligned} \sum_{i=1}^N \tilde{s}_i(\mathbf{w}_i) &= \sum_{i=1}^N s_i(R_i \mathbf{w} - \mathbf{w}_{0,i}) \leq 2 \left(\sum_{i=1}^N s_i(R_i \mathbf{w}) + \sum_{i=1}^N s_i(\mathbf{w}_{0,i}) \right) \\ &= 2 \left(s(\mathbf{w}) + \tilde{s}_0(\mathbf{w}_0) \right) . \end{aligned} \quad (5.9)$$

First from (4.8), then recalling that $C_i \mathbf{w}_{0,i} = C_i R_i \mathbf{w}$ and that by definition (4.6) the $\mathbf{w}_{0,i}$ are local energy minimizers, we get

$$\tilde{s}_0(\mathbf{w}_0) = \sum_{i=1}^N s_i(\mathbf{w}_{0,i}) \leq \sum_{i=1}^N s_i(R_i \mathbf{w}) = s(\mathbf{w}) , \quad (5.10)$$

where we again used (4.3) in the last identity.

Combining bounds (5.9) and (5.10) finally gives (5.5) with $C_0^2 = 5$. \square

LEMMA 5.4. *There exist constants $0 \leq \epsilon_{ij} \leq 1$, $1 \leq i, j \leq N$, such that*

$$|s(R_i^T \mathbf{w}_i, R_j^T \mathbf{w}_j)| \leq \epsilon_{ij} s(R_i^T \mathbf{w}_i) s(R_j^T \mathbf{w}_j) , \quad (5.11)$$

for $\mathbf{w}_i \in \mathbf{W}_i$ and $\mathbf{w}_j \in \mathbf{W}_j$. Denoting the spectral radius of $\mathbb{E} = \{\epsilon_{ij}\}$ by $\rho(\mathbb{E})$, it holds $\rho(\mathbb{E}) \leq 13$.

Proof. The proof is a classical coloring argument and will be presented briefly. Simply, the support of a function $\overline{\mathcal{H}}(R_i^T \mathbf{w}_i)$, $\mathbf{w}_i \in \mathbf{W}_i$, is given by the interior of

$$\bigcup_{j \in \Xi_i} \overline{\Omega}_j \quad (5.12)$$

where Ξ_i is the set of indexes j such that Ω_j shares an edge with Ω_i . Therefore, using a Cauchy-Schwarz inequality, it immediately follows that there exists a matrix $\mathbb{E} = \{\epsilon_{ij}\}$ which satisfies (5.11), each row of which has at most k elements equal to 1, and the remaining terms are zeros. It is easy to check that the integer k is equal to 13 in the quadrilateral case and equal to 10 in the triangular case. As a consequence it holds

$$\rho(\mathbb{E}) \leq \|\mathbb{E}\|_{L^\infty} \leq 13$$

The result is proved. \square

LEMMA 5.5. *There exists $\omega > 0$ such that*

$$s(R_i^T \mathbf{w}_i) \leq \omega \tilde{s}_i(\mathbf{w}_i) \quad \forall \mathbf{w}_i \in \mathbf{W}_i, \quad i = 1, 2, \dots, N; \quad (5.13)$$

$$s(\mathbf{w}_0) \leq \omega \tilde{s}_0(\mathbf{w}_0) \quad \forall \mathbf{w}_0 \in \mathbf{W}_0. \quad (5.14)$$

It holds $\omega = 2(1 + 5k_*^{-1}k^*)$.

Proof. Consider $\mathbf{w}_i \in \mathbf{W}_i$, $i = 1, 2, \dots, N$. By definition (4.4) and recalling that the functions $\mathbf{v}_i \in \mathbf{W}_i$ vanish at the subdomain corner nodes, it is immediate to check that

$$\delta_i \mathbf{v}_i = 2\mathbf{v}_i, \quad \delta_i^\dagger \mathbf{v}_i = \frac{\mathbf{v}_i}{2} \quad \forall \mathbf{v}_i \in \mathbf{W}_i, \quad i = 1, 2, \dots, N. \quad (5.15)$$

Therefore, by definition (4.8) and identity (5.15) it follows

$$\tilde{s}_i(\mathbf{w}_i) = s_i(\delta_i \mathbf{w}_i) = 4 s_i(\mathbf{w}_i). \quad (5.16)$$

Due to (4.3) and definition (4.2) it holds

$$s(R_i^T \mathbf{w}_i) = \sum_{j=1}^N s_j(R_j R_i^T \mathbf{w}_i) = \sum_{j \in \Xi_i} s_j(R_j R_i^T \mathbf{w}_i), \quad (5.17)$$

where Ξ_i was defined after equation (5.12). Consider now $j \in \Xi_i$. If $i = j$, then clearly

$$s_j(R_j R_i^T \mathbf{w}_i) = s_i(\mathbf{w}_i). \quad (5.18)$$

If $i \neq j$, then \mathbf{w}_i is null on all edges of Γ_j excluded Γ_{ij} . Therefore, using (5.2) and (5.3) we get

$$s_j(R_j R_i^T \mathbf{w}_i) \leq k_*^{-1} |R_j R_i^T \mathbf{w}_i|_{\tau(\Gamma_j)}^2 = k_*^{-1} |R_j R_i^T \mathbf{w}_i|_{\tau(\Gamma_{ij})}^2 = k_*^{-1} |\mathbf{w}_i|_{\tau(\Gamma_{ij})}^2, \quad (5.19)$$

which using (5.3) and (5.1) yields

$$s_j(R_j R_i^T \mathbf{w}_i) \leq k_*^{-1} |\mathbf{w}_i|_{\tau(\Gamma_i)}^2 \leq k^* k_*^{-1} s_i(\mathbf{w}_i). \quad (5.20)$$

Combining (5.17) with (5.18), (5.20) and observing that Ω_i has at most four neighbours, gives

$$s(R_i^T \mathbf{w}_i) \leq (1 + 4k^* k_*^{-1}) s_i(\mathbf{w}_i), \quad (5.21)$$

which recalling (5.16) implies

$$s(R_i^T \mathbf{w}_i) \leq (1/4 + k^* k_*^{-1}) \tilde{s}_i(\mathbf{w}_i) . \quad (5.22)$$

Bound (5.13) is proved; we now show (5.14).

First using identity (4.3) and definition (4.6), then with some basic algebra and recalling (4.8), we obtain

$$\begin{aligned} s(\mathbf{w}_0) &= \sum_{i=1}^N s_i(R_i \sum_{j=1}^N R_j^T \delta_j^\dagger \mathbf{w}_{0,j}) \\ &\leq 2 \sum_{i=1}^N \left(s_i(\mathbf{w}_{0,i}) + s_i(\mathbf{w}_{0,i} - R_i \sum_{j=1}^N R_j^T \delta_j^\dagger \mathbf{w}_{0,j}) \right) \\ &= 2 \tilde{s}_0(\mathbf{w}_0) + 2 \sum_{i=1}^N s_i(\mathbf{w}_{0,i} - R_i \sum_{j=1}^N R_j^T \delta_j^\dagger \mathbf{w}_{0,j}) . \end{aligned} \quad (5.23)$$

From (5.7) and the definition of the R_i operators we get

$$\mathbf{w}_{0,i} = R_i \sum_{j=1}^N R_j^T \delta_j^\dagger R_j R_i^T \mathbf{w}_{0,i} . \quad (5.24)$$

As a consequence, it holds

$$\begin{aligned} &\sum_{i=1}^N s_i(\mathbf{w}_{0,i} - R_i \sum_{j=1}^N R_j^T \delta_j^\dagger \mathbf{w}_{0,j}) \\ &= \sum_{i=1}^N s_i(R_i \sum_{j=1}^N R_j^T \delta_j^\dagger (R_j R_i^T \mathbf{w}_{0,i} - \mathbf{w}_{0,j})) . \end{aligned} \quad (5.25)$$

It is easy to check that, for all $i = 1, 2, \dots, N$,

$$R_i \sum_{j=1}^N R_j^T \delta_j^\dagger (R_j R_i^T \mathbf{w}_{0,i} - \mathbf{w}_{0,j}) \in \mathbf{W}_i , \quad (5.26)$$

since it is zero at the nodes of the subdomain corners. For the same reason we also have, for all $j = 1, 2, \dots, N$,

$$(R_j R_i^T \mathbf{w}_{0,i} - \mathbf{w}_{0,j}) \in \mathbf{W}_j . \quad (5.27)$$

Due to (5.26) we can apply bound (5.2) and obtain

$$\begin{aligned} &\sum_{i=1}^N s_i(R_i \sum_{j=1}^N R_j^T \delta_j^\dagger (R_j R_i^T \mathbf{w}_{0,i} - \mathbf{w}_{0,j})) \\ &\leq k_*^{-1} \sum_{i=1}^N |R_i \sum_{j=1}^N R_j^T \delta_j^\dagger (R_j R_i^T \mathbf{w}_{0,i} - \mathbf{w}_{0,j})|_{\tau(\Gamma_i)}^2 \\ &\leq 5 k_*^{-1} \sum_{i=1}^N \sum_{j \in \Xi_i} |R_i R_j^T \delta_j^\dagger (R_j R_i^T \mathbf{w}_{0,i} - \mathbf{w}_{0,j})|_{\tau(\Gamma_i)}^2 , \end{aligned} \quad (5.28)$$

where Ξ_i was defined after equation (5.12). First using property (5.15), then assumption (5.3) and some simple extension-restriction arguments, we get from bound (5.28)

$$\begin{aligned}
& \sum_{i=1}^N s_i \left(R_i \sum_{j \in \Xi_i} R_j^T \delta_j^\dagger (R_j R_i^T \mathbf{w}_{0,i} - \mathbf{w}_{0,j}) \right) \\
& \leq \frac{5}{4k_*} \sum_{i=1}^N \sum_{j \in \Xi_i} |R_i R_j^T (R_j R_i^T \mathbf{w}_{0,i} - \mathbf{w}_{0,j})|_{\tau(\Gamma_i)}^2 \\
& = \frac{5}{4k_*} \sum_{i=1}^N \sum_{j \in \Xi_i, j \neq i} |R_j R_i^T \mathbf{w}_{0,i} - \mathbf{w}_{0,j}|_{\tau(\Gamma_{ij})}^2 \\
& \leq \frac{5}{2k_*} \sum_{i=1}^N \sum_{j \in \Xi_i, j \neq i} |\mathbf{w}_{0,i}|_{\tau(\Gamma_{ij})}^2 + |\mathbf{w}_{0,j}|_{\tau(\Gamma_{ij})}^2 \\
& \leq 5k_*^{-1} \sum_{i=1}^N |\mathbf{w}_{0,i}|_{\tau(\Gamma_i)}^2
\end{aligned} \tag{5.29}$$

Applying (5.1) and using definition (4.8), bound (5.29) gives

$$\begin{aligned}
& \sum_{i=1}^N s_i \left(R_i \sum_{j=1}^N R_j^T \delta_j^\dagger (R_j R_i^T \mathbf{w}_{0,i} - \mathbf{w}_{0,j}) \right) \\
& \leq 5k_*^{-1} k^* \sum_{i=1}^N s_i(\mathbf{w}_{0,i}) = 5k_*^{-1} k^* \tilde{s}_0(\mathbf{w}_0) .
\end{aligned} \tag{5.30}$$

Combining bounds (5.23), (5.25) and (5.30) it finally follows

$$s(\mathbf{w}_0) \leq 2(1 + 5k_*^{-1} k^*) \tilde{s}_0(\mathbf{w}_0) , \tag{5.31}$$

which combined with (5.22) proves the lemma with $\omega = 2(1 + 5k_*^{-1} k^*)$. \square

In Ref. [49] the following result is shown.

THEOREM 5.6. *Let $C_0, \omega, \rho(\mathbb{E})$ be the constants appearing in Lemmata 5.3, 5.4 and 5.5. Then for the condition number of the additive preconditioned operator $P = \sum_{i=0}^N P_i$ it holds*

$$\text{Cond}(P) \leq C_0^2 \omega (\rho(\mathbb{E}) + 1) .$$

Theorem 5.1 follows immediately combining Theorem 5.6 with the bounds in Lemmata 5.3, 5.4 and 5.5.

5.2. Proof of Assumption 5.1. In this section we prove that Assumption 5.1 holds for the MITC plate bending problem (2.4), and show the respective bounds for the constants k_*, k^* .

The local spaces $\overline{\mathbf{W}}_i$, $i = 1, 2, \dots, N$, are composed by rotation and deflection parts, which we indicate in the sequel as

$$\overline{\mathbf{W}}_i = \overline{\Theta}_i \times \overline{U}_i .$$

Accordingly, we indicate the rotation and deflection parts of the constrained space by

$$\mathbf{W}_i = \Theta_i \times U_i ,$$

where the functions of Θ_i and U_i vanish at the subdomain corner nodes. In the sequel, given any $\mathbf{w}_i = (\boldsymbol{\theta}_i, u_i) \in \overline{\mathbf{W}}_i$, we will indicate with $\overline{\mathcal{H}}_i \boldsymbol{\theta}_i$ the rotation part of its energy-harmonic extension $\overline{\mathcal{H}}_i \mathbf{w}_i$ defined in (4.1). Similarly, $\overline{\mathcal{H}}_i u_i$ will represent the deflection part.

Proof of the upper bound (5.1). We start by defining the following edge seminorm on the rotation part

$$|\boldsymbol{\theta}_i|_{\gamma(e)} := \inf_{\boldsymbol{\psi} \in [H^1(\Omega_i)]^2, \boldsymbol{\psi}|_e = \boldsymbol{\theta}_i|_e} \|\boldsymbol{\varepsilon}(\boldsymbol{\psi})\|_{L^2(\Omega_i)} \quad (5.32)$$

for all $e \in \mathcal{E}_i$. Note that, simply restricting the choice in the infimum and since the number of edges of each subdomain is finite, it holds

$$\sum_{e \in \mathcal{E}_i} |\boldsymbol{\theta}_i|_{\gamma(e)}^2 \leq C \inf_{\boldsymbol{\psi} \in [H^1(\Omega_i)]^2, \boldsymbol{\psi}|_{\Gamma_i} = \boldsymbol{\theta}_i} \|\boldsymbol{\varepsilon}(\boldsymbol{\psi})\|_{L^2(\Omega_i)}^2. \quad (5.33)$$

We can now introduce the following seminorm on the space $\overline{\mathbf{W}}_i$:

$$\begin{aligned} |\mathbf{w}_i|_{\tau(\Gamma_i)}^2 &= \sum_{e \in \mathcal{E}_i} |\mathbf{w}_i|_{\tau(e)}^2 \quad \forall \mathbf{w}_i = (\boldsymbol{\theta}_i, u_i) \in \overline{\mathbf{W}}_i, \\ |\mathbf{w}_i|_{\tau(e)}^2 &= |\boldsymbol{\theta}_i|_{\gamma(e)}^2 + ht^{-2} \|\Pi \boldsymbol{\theta}_i \cdot \boldsymbol{\tau} - u'_i\|_{L^2(e)}^2, \end{aligned} \quad (5.34)$$

where $\boldsymbol{\tau}$ is the tangent unit vector at the boundary and the apex indicates as usual the derivative, in the direction of $\boldsymbol{\tau}$, for functions defined on the (one dimensional) boundary. Note that due to property (P6) the operator Π is well defined also when restricted on boundary edges. Norm (5.34) clearly satisfies (5.3) by definition. We will now show the remaining two properties. Consider $\mathbf{w}_i = (\boldsymbol{\theta}_i, u_i) \in \overline{\mathbf{W}}_i$. Using bound (5.33) with the choice $v = \overline{\mathcal{H}}_i \boldsymbol{\theta}_i$, it follows

$$\sum_{e \in \mathcal{E}_i} |\boldsymbol{\theta}_i|_{\gamma(e)}^2 \leq C \|\boldsymbol{\varepsilon}(\overline{\mathcal{H}}_i \boldsymbol{\theta}_i)\|_{L^2(\Omega_i)}^2 \leq 4\alpha^{-1} a_i(\overline{\mathcal{H}}_i \boldsymbol{\theta}_i), \quad (5.35)$$

where $\alpha = \alpha(E, \nu) > 0$ is the coercivity constant for the elastic moduli \mathbb{C} . First recalling (P6) and the definition of gradient, then using Agmon inequality (see [1]) and an inverse estimate we get

$$\begin{aligned} \sum_{e \in \mathcal{E}_i} ht^{-2} \|\Pi \boldsymbol{\theta}_i \cdot \boldsymbol{\tau} - u'_i\|_{L^2(e)}^2 &= \sum_{e \in \mathcal{E}_i} ht^{-2} \|(\Pi \overline{\mathcal{H}}_i \boldsymbol{\theta}_i - \nabla \overline{\mathcal{H}}_i u_i)|_e \cdot \boldsymbol{\tau}\|_{L^2(e)}^2 \\ &\leq Ct^{-2} \|\Pi \overline{\mathcal{H}}_i \boldsymbol{\theta}_i - \nabla \overline{\mathcal{H}}_i u_i\|_{L^2(\Omega_i)}^2, \end{aligned} \quad (5.36)$$

where the constant C depends only on the mesh shape regularity. Finally, combining (5.35) and (5.36) with definition (5.34) we get

$$\begin{aligned} |\mathbf{w}_i|_{\tau(\Gamma_i)}^2 &\leq 4\alpha^{-1} a_i(\overline{\mathcal{H}}_i \boldsymbol{\theta}_i) + Ct^{-2} \|\Pi \overline{\mathcal{H}}_i \boldsymbol{\theta}_i - \nabla \overline{\mathcal{H}}_i u_i\|_{L^2(\Omega_i)}^2 \\ &\leq k^* b_i(\overline{\mathcal{H}}_i \mathbf{w}_i) = k^* s_i(\mathbf{w}_i), \end{aligned} \quad (5.37)$$

where k^* is a new constant depending only on the mesh regularity and material parameters. Assumption (5.1) is proved.

Proof of the lower bound (5.2). Assumption (5.2) is without doubt the more involved; we will make use of the properties (P1)-(P6) already introduced. Consider $\mathbf{w}_i = (\boldsymbol{\theta}_i, u_i) \in \mathbf{W}_i$. In the sequel, Q_i will indicate the restriction of the auxiliary

space Q , introduced in (P5), to the domain Ω_i . We start by solving the following rotated Stokes problem

$$\begin{cases} \text{Find } \tilde{\boldsymbol{\theta}} \in \overline{\boldsymbol{\Theta}}_i, p \in Q_i/\mathbb{R} \text{ s.t.} \\ (\nabla \tilde{\boldsymbol{\theta}}, \nabla \tilde{\boldsymbol{\eta}}) + (p, \text{curl } \boldsymbol{\eta}) = 0 & \forall \boldsymbol{\eta} \in \overline{\boldsymbol{\Theta}}_i \cap [H_0^1(\Omega_i)]^2 \\ (\text{curl } \tilde{\boldsymbol{\theta}}, q) = 0 & \forall q \in Q_i/\mathbb{R} \\ \tilde{\boldsymbol{\theta}} = \boldsymbol{\theta}_i & \text{on } \Gamma_i . \end{cases} \quad (5.38)$$

Due to the stability property (P5), problem (5.38) has a unique solution and, using standard techniques, it can be shown that

$$\|\tilde{\boldsymbol{\theta}}\|_{H^1(\Omega_i)} \leq C \|\boldsymbol{\theta}_i\|_{H^{1/2}(\Gamma_i)} . \quad (5.39)$$

We also define the function $\boldsymbol{\beta} : \Omega_i \rightarrow \mathbb{R}^2$

$$\boldsymbol{\beta}(x, y) = \frac{1}{2|\Omega_i|} [y_b - y, x - x_b]^T \int_{\Omega_i} \text{curl } \tilde{\boldsymbol{\theta}} \quad (5.40)$$

where (x, y) are the standard cartesian coordinates and (x_b, y_b) represents the barycenter of Ω_i . It is immediate to check that

$$\int_{\Omega_i} \text{curl} (\tilde{\boldsymbol{\theta}} - \boldsymbol{\beta}) = 0 , \quad (5.41)$$

and, since $\text{curl } \boldsymbol{\beta}$ is constant,

$$(\text{curl } \boldsymbol{\beta}, q) = 0 \quad \forall q \in Q_i/\mathbb{R} . \quad (5.42)$$

As a consequence of the second identity in problem (5.38) and due to (5.41), (5.42) one has

$$(\text{curl} (\tilde{\boldsymbol{\theta}} - \boldsymbol{\beta}), q) = 0 \quad \forall q \in Q_i, \quad (5.43)$$

i.e.

$$P \text{curl} (\tilde{\boldsymbol{\theta}} - \boldsymbol{\beta}) = 0 , \quad (5.44)$$

where the projection operator P was defined in property (P3). Combining (5.44) with property (P3) we get $\text{curl } \Pi(\tilde{\boldsymbol{\theta}} - \boldsymbol{\beta}) = 0$, which, due to (P4), gives the existence of a function $\Psi \in U|_{\Omega_i}$ such that

$$\Pi(\tilde{\boldsymbol{\theta}} - \boldsymbol{\beta}) = \nabla \Psi . \quad (5.45)$$

Using a standard approximation and scaling argument on Ω_i , we get from (5.40)

$$\|\boldsymbol{\beta}\|_{L^2(\Omega)} \leq \frac{C}{H^2} \|[y_b - y, x - x_b]^T\|_{L^2(\Omega)} \left| \int_{\Omega_i} \text{curl } \tilde{\boldsymbol{\theta}} \right| \leq C \left| \int_{\Omega_i} \text{curl } \tilde{\boldsymbol{\theta}} \right| . \quad (5.46)$$

We now introduce the additional problem

$$\begin{cases} \text{Find } \tilde{u} \in \overline{U}_i \text{ s.t.} \\ (\nabla \tilde{u} - \nabla \Psi, \nabla v) = 0 & \forall v \in \overline{U}_i \cap H_0^1(\Omega_i) \\ \tilde{u} = u_i & \text{on } \Gamma_i . \end{cases} \quad (5.47)$$

Using identity (5.45) and a triangle inequality, then noting that $\boldsymbol{\beta} \in \boldsymbol{\Gamma}$, see [19], we obtain

$$\|\Pi\tilde{\boldsymbol{\theta}} - \nabla\tilde{u}\|_{L^2(\Omega_i)} \leq \|\nabla\Psi - \nabla\tilde{u}\|_{L^2(\Omega_i)} + \|\Pi\boldsymbol{\beta}\|_{L^2(\Omega_i)} = |\Psi - \tilde{u}|_{H^1(\Omega_i)} + \|\boldsymbol{\beta}\|_{L^2(\Omega_i)}. \quad (5.48)$$

Note that by definition (5.47) it holds

$$\tilde{u} - \Psi = \mathcal{H}_i(u_i - \Psi|_{\Gamma_i}), \quad (5.49)$$

with \mathcal{H}_i the standard harmonic extension in the discrete space \overline{U}_i . Moreover, since Ψ is defined up to a constant, we can choose Ψ such that

$$\int_{\Gamma_i} (\Psi|_{\Gamma_i} - u_i) = 0. \quad (5.50)$$

First using (5.49) and well known properties of the discrete Harmonic extension (see for instance [49]), then using (5.50) and a standard scaling argument, we get

$$|\Psi - \tilde{u}|_{H^1(\Omega_i)} \leq C|(\Psi|_{\Gamma_i}) - u_i|_{H^{1/2}(\Gamma_i)} \leq CH^{1/2}\|(\Psi|_{\Gamma_i})' - u_i'\|_{L^2(\Gamma_i)}. \quad (5.51)$$

Recalling (5.45) and due to (5.38) and (P6) it follows

$$(\Psi|_{\Gamma_i})' = \nabla\Psi|_{\Gamma_i} \cdot \boldsymbol{\tau} = \Pi(\tilde{\boldsymbol{\theta}} - \boldsymbol{\beta})|_{\Gamma_i} \cdot \boldsymbol{\tau} = \Pi(\boldsymbol{\theta}_i - \boldsymbol{\beta}|_{\Gamma_i}) \cdot \boldsymbol{\tau}, \quad (5.52)$$

which, using again $\Pi\boldsymbol{\beta} = \boldsymbol{\beta}$, becomes

$$(\Psi|_{\Gamma_i})' = \Pi\boldsymbol{\theta}_i \cdot \boldsymbol{\tau} - \boldsymbol{\beta}|_{\Gamma_i} \cdot \boldsymbol{\tau}. \quad (5.53)$$

Due to (5.51), (5.53) and a triangle inequality

$$|\Psi - \tilde{u}|_{H^1(\Omega_i)} \leq CH^{1/2}\left(\|\Pi\boldsymbol{\theta}_i \cdot \boldsymbol{\tau} - u_i'\|_{L^2(\Gamma_i)} + \|\boldsymbol{\beta}|_{\Gamma_i} \cdot \boldsymbol{\tau}\|_{L^2(\Gamma_i)}\right). \quad (5.54)$$

Using property (P3) and recalling that constant functions are contained in Q_i , an integration by parts easily gives

$$\int_{\Omega_i} \operatorname{curl} \tilde{\boldsymbol{\theta}} = \int_{\Omega_i} \operatorname{curl} \Pi\tilde{\boldsymbol{\theta}} = \int_{\Omega_i} \operatorname{curl} (\Pi\tilde{\boldsymbol{\theta}} - \nabla\tilde{u}) = \int_{\Gamma_i} (\Pi\tilde{\boldsymbol{\theta}} - \nabla\tilde{u}) \cdot \boldsymbol{\tau}. \quad (5.55)$$

Combining (5.46) and (5.55), a standard scaling argument gives

$$\begin{aligned} \|\boldsymbol{\beta}\|_{L^2(\Omega)} &\leq C \int_{\Gamma_i} |(\Pi\tilde{\boldsymbol{\theta}} - \nabla\tilde{u}) \cdot \boldsymbol{\tau}| \leq CH^{1/2}\|(\Pi\tilde{\boldsymbol{\theta}} - \nabla\tilde{u}) \cdot \boldsymbol{\tau}\|_{L^2(\Gamma_i)} \\ &= CH^{1/2}\|\Pi\boldsymbol{\theta}_i - u_i'\|_{L^2(\Gamma_i)}. \end{aligned} \quad (5.56)$$

Using again a scaling argument, the definition of $\boldsymbol{\beta}$ (cf. (5.40)) and (5.56) lead to

$$\|\boldsymbol{\beta}\|_{L^2(\Omega)} + H^{1/2}\|\boldsymbol{\beta}|_{\Gamma_i} \cdot \boldsymbol{\tau}\|_{L^2(\Gamma_i)} \leq C\|\boldsymbol{\beta}\|_{L^2(\Omega)} \leq CH^{1/2}\|\Pi\boldsymbol{\theta}_i - u_i'\|_{L^2(\Gamma_i)}. \quad (5.57)$$

Combining (5.48) with (5.54) and (5.57), we obtain the bound

$$\|\Pi\tilde{\boldsymbol{\theta}} - \nabla\tilde{u}\|_{L^2(\Omega_i)} \leq CH^{1/2}\|\Pi\boldsymbol{\theta}_i - u_i'\|_{L^2(\Gamma_i)}. \quad (5.58)$$

We are now ready to bound $s_i(\mathbf{w}_i)$. By definition, the local energy harmonic extension $\overline{\mathcal{H}}_i \mathbf{w}_i = (\overline{\mathcal{H}}_i \boldsymbol{\theta}_i, \overline{\mathcal{H}}_i u_i)$ is given by

$$\begin{cases} \text{Find } \overline{\mathcal{H}}_i(\mathbf{w}_i) \in \overline{\mathbf{W}}_i \text{ such that:} \\ b_i(\overline{\mathcal{H}}_i \mathbf{w}_i, \mathbf{v}) = 0 \quad \forall \mathbf{v} \in \mathbf{X}_i \\ \overline{\mathcal{H}}_i \mathbf{w}_i|_{\Gamma_i} = \mathbf{w}_i, \end{cases} \quad (5.59)$$

where \mathbf{X}_i is defined in (3.1). Let in the sequel $\tilde{\mathbf{w}} \in \mathbf{X}|_{\Omega_i}$ be given by $\tilde{\mathbf{w}} = (\tilde{\boldsymbol{\theta}}, \tilde{u})$. Note that, due to the definitions (5.38), (5.47) and (5.59) we have

$$\overline{\mathcal{H}}_i \mathbf{w}_i - \tilde{\mathbf{w}} = 0 \quad \text{on } \Gamma_i .$$

Therefore $(\overline{\mathcal{H}}_i \mathbf{w}_i - \tilde{\mathbf{w}}) \in \mathbf{X}_i$ and, due to (5.59), it satisfies

$$b_i(\overline{\mathcal{H}}_i \mathbf{w}_i - \tilde{\mathbf{w}}, \mathbf{v}) = -b_i(\tilde{\mathbf{w}}, \mathbf{v}) \quad \forall \mathbf{v} \in \mathbf{X}_i . \quad (5.60)$$

As a consequence of (5.60) it easily follows

$$b_i(\overline{\mathcal{H}}_i \mathbf{w}_i - \tilde{\mathbf{w}}) \leq b_i(\tilde{\mathbf{w}}) , \quad (5.61)$$

which, recalling the definition of s_i , gives

$$s_i(\mathbf{w}_i) = b_i(\overline{\mathcal{H}}_i \mathbf{w}_i) \leq 4b_i(\tilde{\mathbf{w}}) . \quad (5.62)$$

Therefore, we need to bound

$$\begin{aligned} b_i(\tilde{\mathbf{w}}) &= a_i(\tilde{\boldsymbol{\theta}}) + t^{-2} \|\Pi \tilde{\boldsymbol{\theta}} - \nabla \tilde{u}\|_{L^2(\Omega_i)}^2 \\ &\leq C \|\boldsymbol{\varepsilon}(\tilde{\boldsymbol{\theta}})\|_{L^2(\Omega_i)}^2 + t^{-2} \|\Pi \tilde{\boldsymbol{\theta}} - \nabla \tilde{u}\|_{L^2(\Omega_i)}^2 . \end{aligned} \quad (5.63)$$

From (5.39) we get

$$\|\boldsymbol{\varepsilon}(\tilde{\boldsymbol{\theta}})\|_{L^2(\Omega_i)}^2 \leq |\tilde{\boldsymbol{\theta}}|_{H^1(\Omega_i)}^2 \leq C |\boldsymbol{\theta}_i|_{H^{1/2}(\Gamma_i)} . \quad (5.64)$$

Recalling that $\boldsymbol{\theta}_i$ vanishes at the subdomain corner nodes, we can apply Lemma 7.1 in the Appendix and get from (5.64)

$$\|\boldsymbol{\varepsilon}(\tilde{\boldsymbol{\theta}})\|_{L^2(\Omega_i)}^2 \leq C(1 + \log^2 H/h) \sum_{e \in \mathcal{E}_i} |\boldsymbol{\theta}_i|_{H^{1/2}(e)}^2 . \quad (5.65)$$

Furthermore, using again that $\boldsymbol{\theta}_i$ vanishes at the subdomain corner nodes, we combine Lemma 7.2 in the Appendix (with the choice $s = 2$) and (5.65) in order to obtain

$$\|\boldsymbol{\varepsilon}(\tilde{\boldsymbol{\theta}})\|_{L^2(\Omega_i)}^2 \leq C(H/h)^{1/2} (1 + \log^2 H/h) \sum_{e \in \mathcal{E}_i} |\boldsymbol{\theta}_i|_{\gamma(e)}^2 . \quad (5.66)$$

Finally, joining (5.62), (5.63), (5.66), (5.58) and recalling definition (5.34) it follows

$$\begin{aligned} s_i(\mathbf{w}_i) &\leq C(H/h)^{1/2} (1 + \log^2 H/h) \sum_{e \in \mathcal{E}_i} |\boldsymbol{\theta}_i|_{\gamma(e)}^2 + t^{-2} H \|\Pi \boldsymbol{\theta}_i - u_i'\|_{L^2(\Gamma_i)}^2 \\ &\leq C(H/h) |\mathbf{w}_i|_{\tau(\Gamma_i)}^2 . \end{aligned} \quad (5.67)$$

Bound (5.2) is therefore proved with

$$k_*^{-1} = C(H/h),$$

with the constant C depending only on the material constants and mesh regularity.

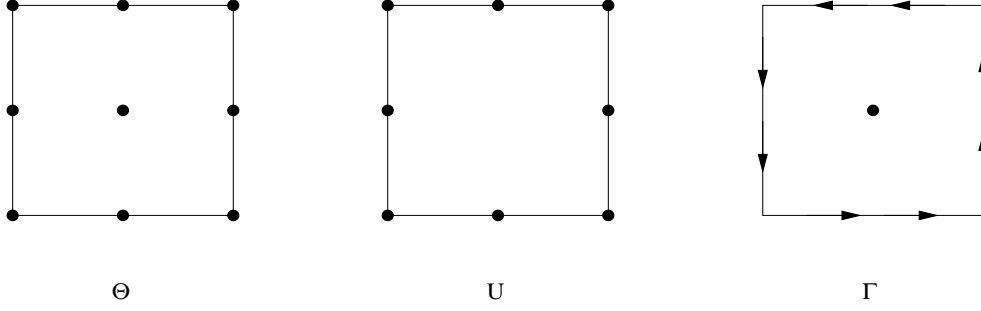


FIG. 6.1. Degrees of freedom for the MITC 9 element

6. Numerical results.

6.1. MITC9 discrete spaces. In the numerical tests, we adopt the MITC 9 quadrilateral element. Since our tests are performed on rectangular meshes, we here briefly summarize the discrete spaces of the MITC 9 only in the simpler rectangular case. A more general description can be found for instance in [8].

Given a rectangular mesh τ_h , let the discrete spaces be defined as

$$\begin{aligned} \Theta &= \{ \boldsymbol{\eta} \in [H_0^1(\Omega)]^2 : \boldsymbol{\eta}|_K \in [\mathcal{Q}_2(K)]^2 \forall K \in \tau_h \}, \\ U &= \{ \boldsymbol{\eta} \in H_0^1(\Omega) : \boldsymbol{\eta}|_K \in \mathcal{Q}_2(K) \cap \mathcal{P}_3(K) \forall K \in \tau_h \}, \end{aligned} \quad (6.1)$$

where $\mathcal{Q}_2(K)$ and $\mathcal{P}_3(K)$ represent respectively the standard spaces of biquadratic polynomials and third order polynomials on the element K .

Moreover, the space Γ is given by

$$\Gamma = \{ \boldsymbol{\gamma} \in H_0(\text{curl}; \Omega) : \boldsymbol{\gamma}|_K \in \text{span}[(1, x, y, xy, y^2) \times (1, x, y, x^2, xy)] \}, \quad (6.2)$$

where x, y are standard cartesian coordinates and $H_0(\text{curl}; \Omega)$ is the space of functions in $[L^2(\Omega)]^2$ with curl in $L^2(\Omega)$ and vanishing tangent component at the boundary.

The operator Π , acting on all $\boldsymbol{\eta} \in [H^1(\Omega)]^2 + \Gamma$, is then defined on every element K by

$$\begin{aligned} \int_l (\boldsymbol{\eta} - \Pi \boldsymbol{\eta}) p_1 &= 0 \quad \forall \text{ edge } l \text{ of } K, \forall p_1 \in \mathcal{P}_1(l), \\ \int_K (\boldsymbol{\eta} - \Pi \boldsymbol{\eta}) &= 0, \end{aligned} \quad (6.3)$$

where $\mathcal{P}_1(l)$ represents the space of the linear polynomials on the edge l . The degrees of freedom for the MITC 9 element are schematically depicted in Figure 6.1. Finally, we note that the auxiliary space Q , which does not appear in the implementation, is simply given by the space of piecewise linear discontinuous functions on τ_h with zero global average.

6.2. Matrix form of the BDDC preconditioner. The BDDC preconditioned operator P defined in (4.11) can be written in matrix form as

$$P = M^{-1} \widehat{S},$$

where M^{-1} is the BDDC preconditioner and \widehat{S} is the Schur complement of the plate stiffness matrix associated with the Schur complement bilinear form (3.3), i.e.

$$s(\boldsymbol{w}_\Gamma, \boldsymbol{v}_\Gamma) = \boldsymbol{w}_\Gamma^T \widehat{S} \boldsymbol{v}_\Gamma.$$

We denote by $K^{(i)}$ the local stiffness matrix of the plate problem (2.4) restricted to subdomain Ω_i . By partitioning the local degrees of freedom into interior (I) and interface (Γ), and by further partitioning the latter into edge (E, also known as dual) and corner (C, also known as primal) degrees of freedom, then $K^{(i)}$ can be written as

$$K^{(i)} = \begin{bmatrix} K_{II}^{(i)} & K_{\Gamma I}^{(i)T} \\ K_{\Gamma I}^{(i)} & K_{\Gamma\Gamma}^{(i)} \end{bmatrix} = \begin{bmatrix} K_{II}^{(i)} & K_{EI}^{(i)T} & K_{CI}^{(i)T} \\ K_{EI}^{(i)} & K_{EE}^{(i)} & K_{CE}^{(i)T} \\ K_{CI}^{(i)} & K_{CE}^{(i)} & K_{CC}^{(i)} \end{bmatrix}.$$

Following the framework of Li and Widlund [34], the BDDC preconditioner can be written as

$$M^{-1} = \tilde{R}_{D,\Gamma}^T \tilde{S}_{\Gamma}^{-1} \tilde{R}_{D,\Gamma}, \quad (6.4)$$

where

$$\tilde{S}_{\Gamma}^{-1} = R_{\Gamma E}^T \left(\sum_{i=1}^N \begin{bmatrix} 0 & R_E^{(i)T} \end{bmatrix} \begin{bmatrix} K_{II}^{(i)} & K_{EI}^{(i)T} \\ K_{EI}^{(i)} & K_{EE}^{(i)} \end{bmatrix}^{-1} \begin{bmatrix} 0 \\ R_E^{(i)} \end{bmatrix} \right) R_{\Gamma E} + \Phi S_{CC}^{-1} \Phi^T. \quad (6.5)$$

The first term in (6.5) is the sum of local solvers on each subdomain Ω_i , defined in (4.10), with Neumann data on the local edges E and with the vertex variables constrained to vanish. The second term is the coarse solve (4.9) for the vertex variables, that we implemented as in [34, 43] using the coarse matrix

$$S_{CC} = \sum_{i=1}^N R_C^{(i)T} \left(K_{CC}^{(i)} - \begin{bmatrix} K_{CI}^{(i)} & K_{CE}^{(i)} \end{bmatrix} \begin{bmatrix} K_{II}^{(i)} & K_{EI}^{(i)T} \\ K_{EI}^{(i)} & K_{EE}^{(i)} \end{bmatrix}^{-1} \begin{bmatrix} K_{CI}^{(i)T} \\ K_{CE}^{(i)T} \end{bmatrix} \right) R_C^{(i)}$$

and a matrix Φ representing a change of variable given by

$$\Phi = R_{\Gamma C}^T - R_{\Gamma E}^T \sum_{i=1}^N \begin{bmatrix} 0 & R_E^{(i)T} \end{bmatrix} \begin{bmatrix} K_{II}^{(i)} & K_{EI}^{(i)T} \\ K_{EI}^{(i)} & K_{EE}^{(i)} \end{bmatrix}^{-1} \begin{bmatrix} K_{CI}^{(i)T} \\ K_{CE}^{(i)T} \end{bmatrix} R_C^{(i)}.$$

The scaled restriction matrix in (6.4) is defined by the direct sum $\tilde{R}_{D,\Gamma} = R_{\Gamma C} \oplus_{i=1}^N R_{D,E}^{(i)} R_{\Gamma E}$ and we refer to [34, 43] for a detailed description of the other restriction and interpolation matrices.

6.3. Numerical tests. The discrete Reissner-Mindlin plate problem (3.4) is solved iteratively by PCG with the BDDC preconditioner described before. The plate midsurface Ω is the reference square, subdivided into $\sqrt{N} \times \sqrt{N}$ square subdomains of characteristic size H . The algorithm has been implemented in Matlab, the initial guess is always zero, the right hand side is a uniform unitary load, and the stopping criterion is $\|r_k\|_2 / \|r_0\|_2 \leq 10^{-6}$, where r_k is the residual at the k -th iterate. In all our tests, the minimum eigenvalue λ_{min} of the BDDC preconditioned operator was always very close to one ($1 \leq \lambda_{min} \leq 1 + 7 \cdot 10^{-3}$). Therefore, in all our BDDC results, we will report for brevity only the maximum eigenvalue λ_{MAX} , which is essentially equal to the condition number.

Ill-conditioning of the original discrete Reissner-Mindlin plate problem. We report first in Fig. 6.2 the condition number estimates, computed with the Matlab function `condst(\cdot)` of the unpreconditioned discrete Reissner-Mindlin plate

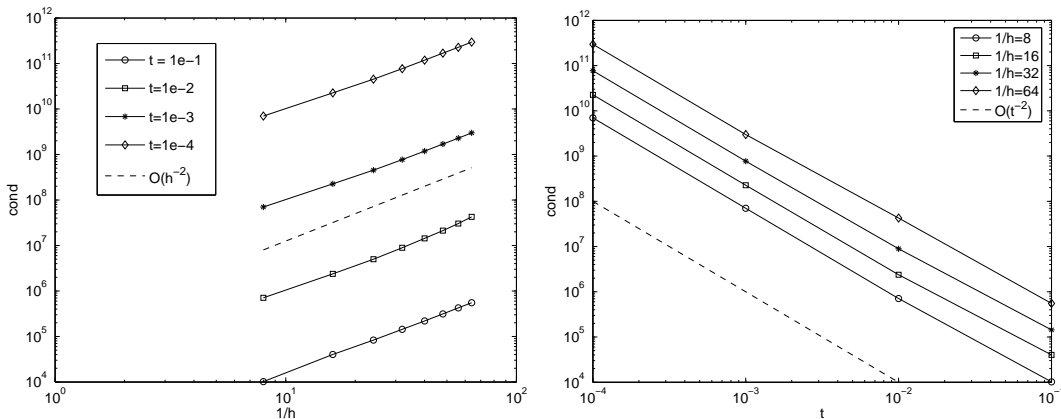


FIG. 6.2. Conditioning of the discrete Reissner-Mindlin plate problem discretized with MITC9 plate elements as a function of $1/h$ (left) and as a function of t (right).

problem discretized with MITC9 plate elements. The left panel shows the loglog plot of the condition number estimates as a function of $1/h$ for given values of t : the comparison with the reference dashed line indicates that, after an initial slower growth, the condition numbers seem to settle toward an $O(h^{-2})$ growth. The right panel shows the loglog plot of the condition number as a function of t for given values of $1/h$: the comparison with the reference dashed line indicates an $O(t^{-2})$ growth.

BDDC scalability. Table 6.1 reports the results of a scalability test for BDDC where the number of subdomains N is increased from 4 to 576 and the mesh size is decreased proportionally from $h = 1/8$ to $1/96$, so that the subdomain size is kept fixed, since $H/h = 4$. Four different values $t = 10^{-1}, 10^{-2}, 10^{-3}, 10^{-4}$ are considered in four different columns. In each case, the results show that λ_{MAX} is bounded from above when N increases, i.e. our BDDC plate algorithm is scalable in complete accordance with the theoretical results of Theorem 5.2. The corresponding iteration counts are also bounded from above for $t = 10^{-1}$, while for smaller values of t they still exhibit a slight growth probably due to N not being sufficiently large. The values of λ_{max} from Table 6.1 are plotted in Fig. 6.3, left panel, while the right panel shows the scalability results for the two values $H/h = 2, 4$ fixing the plate thickness to $t = 10^{-3}$.

BDDC quasi-optimality. Fig. 6.4 displays λ_{MAX} as a function of the ratio H/h when the number of subdomains $N = 4 \times 4$ is kept fixed. Three different values of $t = 10^{-1}, 10^{-2}, 10^{-3}$ are considered. In each case, the plots indicate a (poly)logarithmic growth of λ_{MAX} , hence of the condition number. The behavior of the method with respect to the ratio H/h seems therefore to be better than the theory prediction, at least for the considered test based on a simplified plate geometry and decomposition into subdomains. This subtle point and the influence of complex geometries will be the subject of future research.

BDDC robustness in t . In Fig. 6.5, the values of λ_{MAX} are plotted as a function of t for three cases from Table 6.1 ($1/h = 16, 32, 64$). The results show clearly the independence on t of the BDDC condition number: after an initial growth in going from $t = 10^{-1}$ to $t = 10^{-2}$, λ_{MAX} decreases and settles to a constant value with decreasing t , again in full agreement with the developed theory.

BDDC robustness with respect to jump discontinuities of the plate coefficients. In Fig. 6.6, we consider a plate problem with increasing jump discontinu-

TABLE 6.1

BDDC scalability: maximum eigenvalue λ_{MAX} and iteration counts *it.* for increasing number of subdomains N of fixed size $H/h = 4$ and $t = 10^{-1}, 10^{-2}, 10^{-3}, 10^{-4}$.

$1/h$	N	$t = 10^{-1}$		$t = 10^{-2}$		$t = 10^{-3}$		$t = 10^{-4}$	
		λ_{MAX}	it.	λ_{MAX}	it.	λ_{MAX}	it.	λ_{MAX}	it.
8	$4 = 2 \times 2$	1.978	6	2.075	7	2.078	7	2.438	8
16	$16 = 4 \times 4$	5.333	10	6.230	12	6.180	13	6.179	17
24	$36 = 6 \times 6$	5.755	13	8.137	16	7.729	18	7.723	20
32	$64 = 8 \times 8$	5.290	15	9.123	19	8.419	21	8.405	23
48	$144 = 12 \times 12$	4.924	16	10.008	23	8.949	24	8.920	26
64	$256 = 16 \times 16$	4.920	16	10.219	27	9.165	27	9.102	28
96	$576 = 24 \times 24$	5.001	17	9.790	29	9.352	28	9.214	30

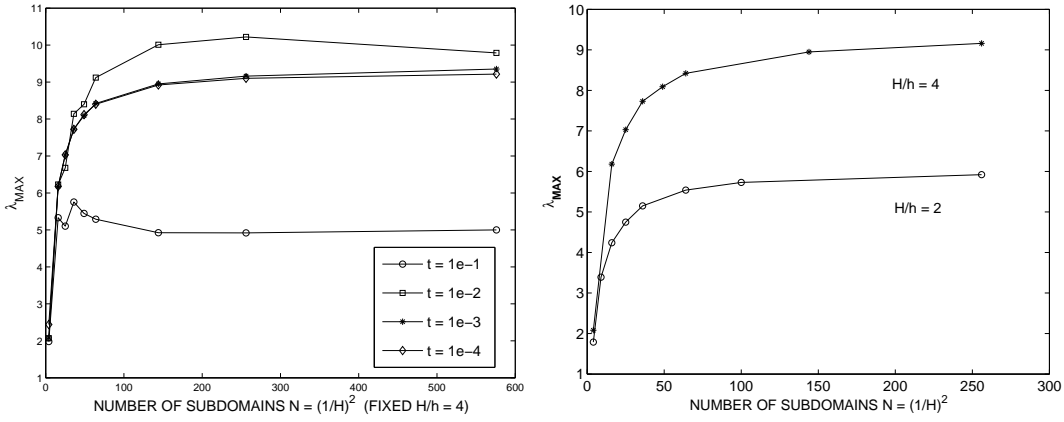


FIG. 6.3. BDDC scalability: maximum eigenvalue λ_{MAX} as a function of N for different values of t , fixed $H/h = 4$ (left, from Table 6.1) and for different values of H/h , fixed $t = 10^{-3}$ (right).

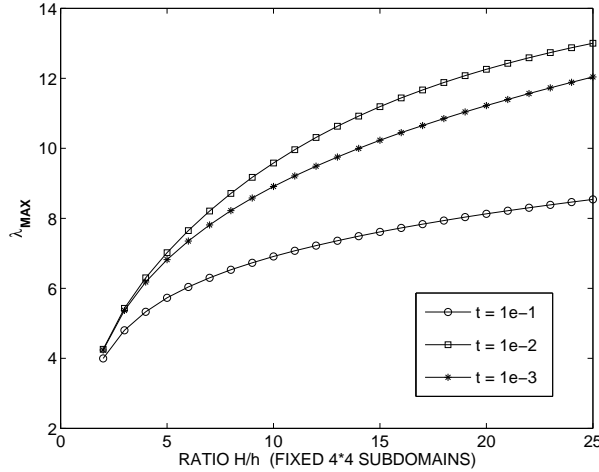


FIG. 6.4. BDDC quasi-optimality: maximum eigenvalue λ_{MAX} as a function of H/h for fixed number of subdomains $N = 4 \times 4$ and $t = 10^{-1}, 10^{-2}, 10^{-3}$.

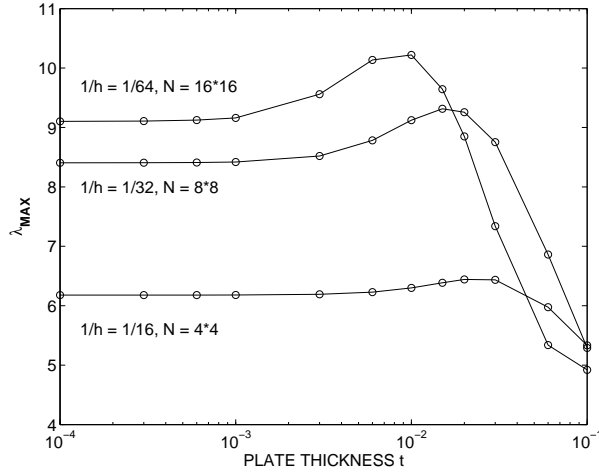


FIG. 6.5. BDDC robustness in t : maximum eigenvalue λ_{MAX} as a function of t for different choices of h and N .

ities in Young's modulus across subdomain boundaries, for fixed $h = 1/64$, $N = 4 \times 4$. As depicted in the top left panel, Young's modulus E is changed to ρE , where the coefficient ρ is fixed to one in the boundary subdomains but it is varied by 8 orders of magnitude from $\rho = 10^{-4}$ to 10^4 in the 2×2 interior subdomains. The table in the bottom panel reports λ_{MAX} and the iteration counts it. for increasing discontinuity jump ρE and decreasing values of plate thickness $t = 10^{-1}, 10^{-2}, 10^{-3}, 10^{-4}$, in different columns. The case denoted by - in the table could not be run due to excessive rounding errors. The same values of λ_{MAX} are plotted in the top right figure as a function of ρ , on a logarithmic scale. These results clearly show the robustness of our BDDC plate algorithm with respect to the jump discontinuities in ρE up to 8 orders of magnitude. We also remark that without the BDDC preconditioner, unpreconditioned CG failed to converge in the tests with largest jumps.

7. Appendix: two technical Lemmata. In this Appendix we will indicate with $\omega \subset \mathbb{R}^2$ a convex quadrilateral or triangular domain of characteristic size H and with \mathcal{E} the set of its edges. Moreover \mathbf{V}_h will represent a continuous finite element space of functions $\partial\omega \rightarrow \mathbb{R}^2$. Finally, h will indicate the characteristic size of the mesh defining \mathbf{V}_h , and we will assume that the functions of \mathbf{V}_h vanish at the corners of ω .

The proof of the following Lemma is not shown since it follows easily, for instance, from analogous results in [49].

LEMMA 7.1. *It holds*

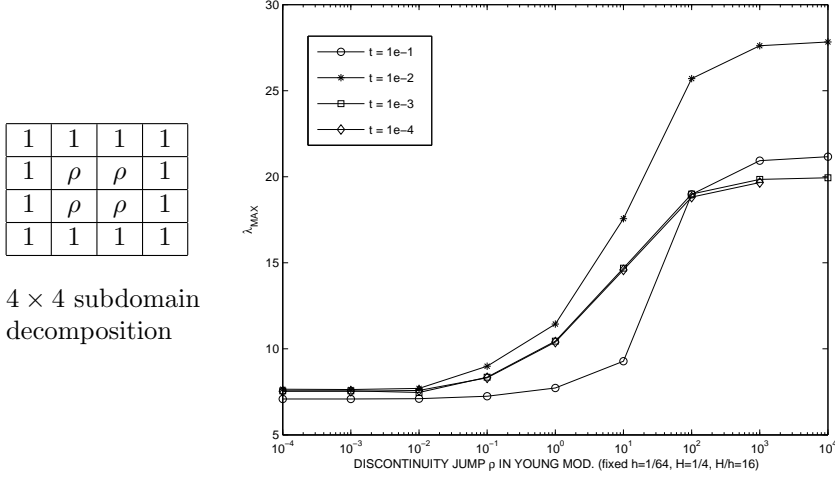
$$|\mathbf{v}|_{H^{1/2}(\partial\omega)}^2 \leq C(1 + \log^2 H/h) \sum_{e \in \mathcal{E}} |\mathbf{v}|_{H^{1/2}(e)}^2 \quad \forall \mathbf{v} \in \mathbf{V}_h,$$

where the constant C depends only on the shape regularity of ω , the shape regularity of the mesh and the polynomial degree of \mathbf{V}_h .

We also have

LEMMA 7.2. *For any real number $s > 0$ it holds*

$$|\mathbf{v}|_{H^{1/2}(e)}^2 \leq C_s (H/h)^{\frac{s}{2+s}} |\mathbf{v}|_{\gamma(e)}^2 \quad \forall \mathbf{v} \in \mathbf{V}_h, \quad \forall e \in \mathcal{E},$$



ρ	$t = 10^{-1}$		$t = 10^{-2}$		$t = 10^{-3}$		$t = 10^{-4}$	
	λ_{MAX}	it.	λ_{MAX}	it.	λ_{MAX}	it.	λ_{MAX}	it.
10^{-4}	7.084	12	7.652	15	7.561	16	7.533	19
10^{-3}	7.086	12	7.635	15	7.559	16	7.537	19
10^{-2}	7.103	12	7.700	14	7.461	16	7.579	18
10^{-1}	7.243	12	8.991	15	8.350	17	8.316	19
1	7.727	12	11.440	17	10.447	18	10.391	21
10	9.280	12	17.564	17	14.689	19	14.587	24
10^2	18.974	13	25.700	18	18.996	21	18.818	26
10^3	20.933	14	27.611	19	19.848	21	19.665	28
10^4	21.167	15	27.829	21	19.942	20	-	-

FIG. 6.6. BBDC robustness with respect to jump discontinuities in Young's modulus ρE . Top left: 4×4 subdomain decomposition of Ω with $\rho = 10^{-4}, \dots, 10^4$ in the 2×2 interior subdomains while $\rho = 1$ in the boundary subdomains. Top right: plot of the data for λ_{MAX} in the table below. Bottom: table with maximum eigenvalue λ_{MAX} and iteration counts *it.* for increasing discontinuity jump ρE and decreasing plate thickness $t = 10^{-1}, 10^{-2}, 10^{-3}, 10^{-4}$, for fixed mesh size $h = 1/64$, number of subdomains $N = 4 \times 4$, subdomain size $H/h = 16$.

where the seminorm $|\cdot|_{\gamma(e)}$ is defined in (5.32). The constant C_s depends only on s , the shape regularity of ω , the shape regularity of the mesh and the polynomial degree of \mathbf{V}_h . Furthermore, $C_s \rightarrow +\infty$ as $s \rightarrow 0_+$.

Proof. Consider $e \in \mathcal{E}$. By the definition of the $H^{1/2}(e)$ -norm, definition (5.34) and due to the dense inclusion $C^\infty(\omega) \subset H^1(\Omega)$, it is sufficient to show that it holds

$$\inf_{\psi \in [C^\infty(\omega)]^2, \psi|_e = \mathbf{v}|_e} \|\nabla \psi\|_{L^2(\omega)} \leq C_s \inf_{\psi \in [C^\infty(\omega)]^2, \psi|_e = \mathbf{v}|_e} \|\varepsilon(\psi)\|_{L^2(\omega)} \quad (7.1)$$

for all $\mathbf{v} \in \mathbf{V}_h$. It is easy to check that (7.1) is implied by

$$\|\nabla \psi\|_{L^2(\omega)} \leq C_s \|\varepsilon(\psi)\|_{L^2(\omega)} \quad (7.2)$$

for all $\psi \in [C^\infty(\omega)]^2$ vanishing at the two endpoints of e .

Due to Lemma 4 in [31] we have

$$\inf_{\bar{\psi} \in R} \|\nabla(\psi + \bar{\psi})\|_{L^2(\omega)} \leq C \|\varepsilon(\psi)\|_{L^2(\omega)}, \quad (7.3)$$

where R denotes the set of rigid body motions of ω . By definition, any $\bar{\psi} \in R$ can be written as

$$\bar{\psi}(x, y) = \mathbf{c} + \beta[-y, x]^T, \quad \mathbf{c} \in \mathbb{R}^2, \quad \beta \in \mathbb{R}, \quad (7.4)$$

where x, y are the standard cartesian coordinates. It holds

$$\|\nabla \bar{\psi}\|_{L^2(\omega)} \leq C |\beta| H. \quad (7.5)$$

Let now $\nu = (\nu_x, \nu_y)$ and $\nu' = (\nu'_x, \nu'_y)$ denote the two endpoints of the edge e . From (7.4) it easily follows

$$|\beta| = \frac{\|\bar{\psi}(\nu) - \bar{\psi}(\nu')\|}{\|[\nu'_y - \nu_y, \nu_x - \nu'_x]^T\|} \leq \frac{C}{H} \|\bar{\psi}(\nu) - \bar{\psi}(\nu')\|, \quad (7.6)$$

where $\|\cdot\|$ indicates the l_1 norm

$$\|\varphi\| = |\varphi_1| + |\varphi_2| \quad \forall \varphi = [\varphi_1, \varphi_2]^T \in \mathbb{R}^2.$$

Observing that $\psi(\nu) = \psi(\nu') = 0$, from (7.6) and the fundamental theorem of calculus, we get

$$|\beta| \leq \frac{C}{H} \|(\bar{\psi}(\nu) + \psi(\nu)) - (\bar{\psi}(\nu') + \psi(\nu'))\| = \frac{C}{H} \left\| \int_e [\nabla(\bar{\psi} + \psi)] \boldsymbol{\tau} \right\|, \quad (7.7)$$

where $\boldsymbol{\tau}$ is as usual the tangent unit vector. First joining (7.5) and (7.7), then using the techniques in Lemma 4.1 of [20], for any $s > 0$ we obtain

$$\|\nabla \bar{\psi}\|_{L^2(\omega)} \leq C \left\| \int_e [\nabla(\bar{\psi} + \psi)] \boldsymbol{\tau} \right\| \leq C_s H^{\frac{s}{2+s}} \|\nabla(\bar{\psi} + \psi)\|_{L^{2+s}(\omega)} \quad \forall \bar{\psi} \in R, \quad (7.8)$$

where the constant $C(s)$ depends on s and blows up as $s \rightarrow 0_+$. Taking the infimum in (7.8) and using an inverse estimate it now follows

$$\inf_{\bar{\psi} \in R} \|\nabla \bar{\psi}\|_{L^2(\omega)} \leq C(s) (H/h)^{\frac{s}{2+s}} \inf_{\bar{\psi} \in R} \|\nabla(\bar{\psi} + \psi)\|_{L^2(\omega)}. \quad (7.9)$$

By the triangle inequality, a combination of (7.9) and (7.3), we finally have

$$\begin{aligned} \|\nabla \psi\|_{L^2(\omega)} &\leq \inf_{\bar{\psi} \in R} \left(\|\nabla(\psi + \bar{\psi})\|_{L^2(\omega)} + \|\nabla \bar{\psi}\|_{L^2(\omega)} \right) \\ &\leq C_s (H/h)^{\frac{s}{2+s}} \|\boldsymbol{\varepsilon}(\psi)\|_{L^2(\omega)}. \end{aligned} \quad (7.10)$$

REFERENCES

- [1] S. Agmon, *Lectures on elliptic boundary value problems*, Van Nostrand Mathematical Studies, Princeton, NJ, 1965.
- [2] D.N. Arnold, and R.S. Falk, *A uniformly accurate finite element method for the Reissner-Mindlin plate*, SIAM J. Numer. Anal., 26: 1276–1290, 1989.
- [3] D.N. Arnold and R.S. Falk, *The boundary layer for the Reissner-Mindlin plate model*, SIAM J. Math. Anal., 21: 281–312, 1990.
- [4] D.N. Arnold and R.S. Falk, *Asymptotic analysis of the boundary layer for the Reissner-Mindlin plate model*, SIAM J. Math. Anal., 27: 486–514, 1996.
- [5] D. N. Arnold, R. S. Falk and R. Winther, *Preconditioning discrete approximations of the Reissner-Mindlin plate model*, Math. Mod. Numer. Anal., 31 (4): 517–557, 1997.

- [6] F. Auricchio, and C. Lovadina, *Analysis of kinematic linked interpolation methods for Reissner-Mindlin plate problems*, Comput. Methods Appl. Mech. Engrg., 190: 2465–2482, 2001.
- [7] F. Auricchio, and C. Lovadina, *Partial selective reduced integration schemes and kinematically linked interpolations for plate bending problems*, Math. Models Methods Appl. Sci., 9: 693–722, 1999.
- [8] K.J. Bathe, *Finite Element Procedures in Engineering Analysis*, Prentice-Hall, Englewood Cliffs, NJ, 1982.
- [9] K.J. Bathe, F. Brezzi and M. Fortin, *Mixed-interpolated elements for the Reissner-Mindlin plates*, Int. J. Num. Meth. Engrg., 28: 1787–1801, 1989.
- [10] L. Beirão da Veiga, *Finite element methods for a modified Reissner-Mindlin free plate model*, SIAM J. Num. Anal., 42: 1572–1591, 2004.
- [11] L. Beirão da Veiga, *Optimal error bounds for the MITC₄ plate bending element*, Calcolo, 41: 227–245, 2004.
- [12] L. Beirão da Veiga, C. Lovadina and L.F. Pavarino, *Positive definite Balancing Neumann-Neumann preconditioners for nearly incompressible elasticity*, Numer. Math. 104: 271–296, 2006.
- [13] S. C. Brenner and L.-Y. Sung, *Balancing domain decomposition for nonconforming plate elements*, Numer. Math., 83: 25–52, 1999.
- [14] S. C. Brenner and L.-Y. Sung, *Two-level additive Schwarz preconditioners for C^0 interior penalty methods*, Numer. Math., 102: 231–255, 2005.
- [15] S. C. Brenner and L.-Y. Sung, *Multigrid algorithms for C^0 interior penalty methods*, SIAM J. Numer. Anal., 44 (1): 199–223, 2006.
- [16] S. C. Brenner and L.-Y. Sung, *BBDC and FETI-DP without matrices or vectors*, Comput. Meth. Appl. Mech. Engrg., 196 (8): 1429–1435, 2007.
- [17] F. Brezzi, K.J. Bathe, and M. Fortin, *Mixed-interpolated elements for Reissner-Mindlin plates*, Internat. J. Numer. Methods Engrg., 28: 1787–1801, 1989.
- [18] F. Brezzi, and M. Fortin, *Mixed and Hybrid Finite Element Methods*, Springer, New York, 1991.
- [19] F. Brezzi, M. Fortin and R. Stenberg, *Error analysis of mixed-interpolated elements for Reissner-Mindlin plates*, Math. Models Meth. Appl. Sci., 1: 125–151, 1991.
- [20] F. Brezzi, K. Lipnikov and M. Shashkov, *Convergence of mimetic finite difference methods for diffusion problems on polyhedral meshes*, SIAM J. Num. Anal., 43: 1872–1896, 2005.
- [21] D. Chapelle, and R. Stenberg, *An optimal low-order locking-free finite element method for Reissner-Mindlin plates*, Math. Models and Methods in Appl. Sci., 8: 407–430, 1998.
- [22] C. Chinosi, C. Lovadina and L. D. Marini, *Nonconforming locking-free finite elements for Reissner-Mindlin plates*, Comput. Meth. Appl. Mech. Engrg., 195 (25-28): 3448–3460, 2006.
- [23] C.R. Dohrmann, *A Preconditioner for Substructuring Based on Constrained Energy Minimization*, SIAM J. Sci.Comp., 25: 246–258, 2003.
- [24] C.R. Dohrmann, *Preconditioning of saddle point systems by substructuring and a penalty approach*, in Domain Decomposition Methods in Science and Engineering XVI, LNCSE 55, O.B. Widlund and D. Keyes, eds., pp. 53–64, Springer, 2006.
- [25] C.R. Dohrmann, *A substructuring preconditioner for nearly incompressible elasticity problems*, Tech. Rep. SAND2004-5393, Sandia National Laboratories, Albuquerque, NM, 2004.
- [26] R. Duran and E. Liberman, *On mixed finite element methods for the Reissner-Mindlin plate model*, Math. Comp., 58: 561–573, 1992.
- [27] R. Duran, E. Hernandez, L. Hervella-Nieto, E. Liberman and R. Rodriguez, *Error estimates for low-order isoparametric quadrilateral finite elements for plates*, SIAM J. Numer. Anal., 41: 1751–1772, 2003.
- [28] C. Farhat, M. Leisoine, P. Le Tallec, K. Pierson and D. Rixen. *FETI-DP: A dual-primal unified FETI method - part I: A faster alternative to the two-level FETI method*, Inter. J. Numer. Meth. Engrg., 50: 1523–1544, 2001.
- [29] R.S. Falk, and T. Tu, *Locking-free finite elements for the Reissner-Mindlin plate*, Math. Comp., 69: 911–928, 2000.
- [30] P. Goldfeld, L. F. Pavarino, and O. B. Widlund, *Balancing Neumann-Neumann preconditioners for mixed approximations of heterogeneous problems in linear elasticity*, Numer. Math., 95(2): 283–324, 2003.
- [31] A. Klawonn and O. Widlund, *A domain decomposition method with Lagrange multipliers and inexact solvers for linear elasticity*, SIAM J. Sci. Comp. 22: 1199–1219, 2000.
- [32] A. Klawonn and O. Widlund, *Dual-primal FETI methods for linear elasticity*, Comm. Pure Appl. Math., 59: 1523–1572, 2006.
- [33] P. Le Tallec, J. Mandel and M. Vidrascu, *A Neumann-Neumann domain decomposition al-*

- gorithm for solving plate and shell problems*, SIAM J. Numer. Anal., 35 (2): 836–967, 1998.
- [34] J. Li and O. B. Widlund, *FETI-DP, BDDC, and block Cholesky methods*, Int. J. Numer. Meth. Engrg., 66 (2): 250–271, 2006.
- [35] J. Li and O. B. Widlund, *BDDC algorithms for incompressible Stokes equations*, SIAM J. Numer. Anal., 44 (6): 2432–2455, 2006.
- [36] C. Lovadina, *A low-order nonconforming finite element for Reissner-Mindlin plates*, SIAM J. Numer. Anal., 42 (6): 2688–2705, 2005.
- [37] C. Lovadina, *A new class of mixed finite element methods for Reissner-Mindlin plates*, SIAM J. Numer. Anal., 33: 2457–2467, 1996.
- [38] C. Lovadina, *Analysis of a mixed finite element method for the Reissner-Mindlin plate problems*, Comput. Methods Appl. Mech. Engrg., 163: 71–85, 1998.
- [39] M. Lyly, *On the connection between some linear triangular Reissner-Mindlin plate bending elements*, Numer. Math., 85: 77–107, 2000.
- [40] J. Mandel, C.R. Dohrmann, *Convergence of a balancing domain decomposition by constraints and energy minimization*, Num. Lin. Alg. Appl., 10: 639–659, 2003.
- [41] J. Mandel, C. R. Dohrmann and R. Tezaur, *An algebraic theory for primal and dual substructuring methods by constraints*, Appl. Numer. Math., 54 (2): 167–193, 2005.
- [42] L. Marcinkowski, *Domain decomposition methods for mortar finite element discretizations of plate problems*, SIAM J. Numer. Anal., 39 (4): 1097–1114, 2001.
- [43] L. F. Pavarino, *BDDC and FETI-DP preconditioners for spectral element discretizations*, Comput. Meth. Appl. Mech. Engrg., 196 (8): 1380–1388, 2007.
- [44] L. F. Pavarino and O. B. Widlund, *Balancing Neumann-Neumann methods for incompressible Stokes equations*, Comm. Pure Appl. Math., 55(3): 302–335, 2002.
- [45] J. Pitkäranta and M. Suri, *Upper and lower error bounds for plate-bending finite elements*, Numer. Math., 84: 611–648, 2000.
- [46] R. Stenberg, *A new finite element formulation for the plate bending problem*, in Asymptotic Methods for Elastic Structures, eds. P.G. Ciarlet, L. Trabucho and J. Viaño, Walter de Gruyter & Co.
- [47] R.L. Taylor, and F. Auricchio, *Linked interpolation for Reissner-Mindlin plate elements: Part II- A simple triangle*, Int. J. Numer. Methods Eng., 36: 3057–3066, 1993.
- [48] A. Tessler and T.J.R. Hughes, *A three-node Mindlin plate element with improved transverse shear*, Comput. Methods Appl. Mech. Engrg., 50: 1–101, 1985.
- [49] A. Toselli and O. B. Widlund, *Domain Decomposition Methods - Algorithms and Theory*, Springer Series in Computational Mathematics, Vol. 34, 2005.
- [50] X. Tu, *BDDC domain decomposition algorithms: methods with three levels and for flow in porous media*, Ph.D. thesis, Department of Computer Science, Courant Institute of Mathematical Sciences, New York, 2006.
- [51] X. Tu, *A BDDC algorithm for a mixed formulation of flow in porous media*, Electron. Trans. Numer. Anal., 20: 64–179, 2005.